Progress In Electromagnetics Research Letters, Vol. 107, 49–57, 2022

Light-Weight Unmanned Aerial Vehicle Wireless Power Transfer System Based on Hollow Copper Coated Aluminum Tubes

Pengcheng Cao[1], Yong Lu[1], Changbo Lu[2], and Shuai Wu[3, *]

Abstract—Limited endurance has become a bottleneck restricting the wide application of unmanned aerial vehicles (UAVs), and wireless power transfer (WPT) technology is expected to become an effective means to help UAVs break this bottleneck. UAV has strict restrictions on the weight of onboard system, so the lightweight design of the receiving side has become the core goal of UAV WPT systems design. In order to achieve this goal, this paper first proposes a novel magnetic coupler based on hollow copper-coated aluminum tubes, in which the receivers act as both landing gears and energy pick-up. The coupling mechanism of the magnetic coupler is analyzed. Secondly, based on the LCC-S resonant compensation network with a simple structure on the receiving-side, the system circuit is designed, and the system transmission model is established. Finally, a UAV WPT prototype is built and tested. The experimental results show that the transmission power of the designed system can reach 157 W, the overall efficiency 80%, and each receiver (also acting as landing gear) weight only 22 g. The weight power density ratio is 3.568 W/g.

1. INTRODUCTION

With the development of automation technology, unmanned aerial vehicle (UAV) is becoming more and more mature and has shown great prospects for applications in many fields such as patrol inspection, rescue, and transportation [1–3]. However, the flight time of UAV is usually only about 30 minutes, which seriously limits the further popularization and application of UAV.

As an emerging technology that can realize power transmission without the need for physical contact, wireless power transfer (WPT) is safe and convenient. Therefore, it has been used in various situations, such as wireless charging of electric vehicles [4, 5], underwater vehicles [6, 7], and automated guided vehicles [8]. With such attractive features, WPT technology becomes a promising candidate to help UAV break through the development dilemma.

In order to realize the wireless charging for UAVs, much research has been conducted. In [9], a UAV WPT system with a disk coil to spiral coil magnetic structure is developed. The spiral coil on the receiving side is installed on the UAV fuselage. The system can transmit the power of 10 W with an efficiency of 93.6%. In [10], an air-core coil replaces the original propeller guard to realize 13 W power transmission, with an efficiency of 60%. In [11], a 500 W UAV WPT system with an efficiency of 91.9% is reported, in which a disk-shaped receiving coil is placed at the bottom of the UAV fuselage. References [12–14] use similar disk-to-disk magnetic structures to design UAV systems. Meanwhile, [15–17] also put forward the idea of using metal tubes to realize the lightweight design of receivers. This magnetic structure has been proved to be suitable for various power level applications. Unfortunately, this disk-to-disk magnetic structure has been proved to produce great magnetic leakage which causes system power loss [18], having a serious adverse impact on the safety of UAV.

Received 16 August 2022, Accepted 11 October 2022, Scheduled 20 October 2022
* Corresponding author: Shuai Wu (wushuai@hit.edu.cn).
[1] School of Power and Energy Engineering, Harbin Engineering University, Harbin, China. [2] Institution of System Engineering, Academy of Military Sciences, China. [3] School of New Energy, Harbin Institute of Technology, Weihai, China.

To reduce magnetic flux leakage, Park et al. [19] try to install the receiving coil at the bottom of the landing gear, so as to reduce the height of the magnetic field operation space as much as possible to ensure electromagnetic safety. Song et al. [20] design a three-phase tightly coupled WPT system for UAV. This system can limit the magnetic field in a small space and basically has no electromagnetic interference problem. However, both systems mentioned above need to use ferrite. Fragile ferrite is easily broken during UAV landing [21].

For the purpose of improving coupling capacity and reducing interference due to leakage magnetic flux, the authors have proposed an orthogonal magnetic structure for UAV WPT applications [22, 23], which can be easily installed on the landing gear of UAV. With in-depth research, the authors realize that the structure has room for improvement in lightweight design. If a structural element of UAV can be used as the receiving coil instead of installing an extra receiver coil wound by litz wire, the weight of the receiver can be effectively reduced. Based on this idea, this paper presents a novel high power density coupling structure for UAV wireless charging. Compared with the previous work [16], two landing gears made of hollow copper-coated aluminum tubes are really used as receiving coils, and transmission power density is increased by orthogonal magnetic coupling structure. On the premise of hardly increasing the additional load of the UAV, the wireless power transmission to the UAV is realized with high weight power density.

The remainder of the article is arranged as follows. In Section 2, the novel magnetic structure is presented. The circuit design and analysis are detailed in Section 3. Section 4 presents the construction and test of experimental prototype. Finally, Section 5 briefly concludes this article.

2. THE NOVEL MAGNETIC COUPLER BASED ON HOLLOW COPPER COATED ALUMINUM TUBES

2.1. Overall System Structure

The proposed magnetic coupler is shown in Fig. 1, and the whole system includes two identical parallel channels. Channel 1 consists of Transmitter 1 and Receiver 1, and Channel 2 consists of Transmitter 2 and Receiver 2. Receiver 1 and Receiver 2 are the two landing gears of UAV. The magnetic structures and parameters of the two channels are identical. It should be mentioned that the misalignment problem of UAV can be solved by simple auxiliary mechanical alignment equipment, so the misalignment problem will not be considered in this paper.

As shown in Fig. 2, the two transmitters are linked in series, so as to simplify the complexity of driving circuit topology. Based on DC-input, inverter, and resonant compensation network, high-

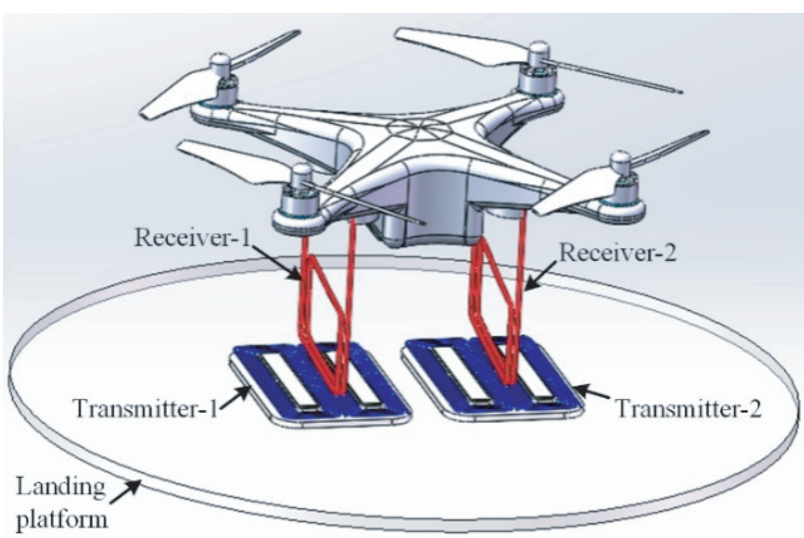

Figure 1. Installation and application diagram of the whole system.

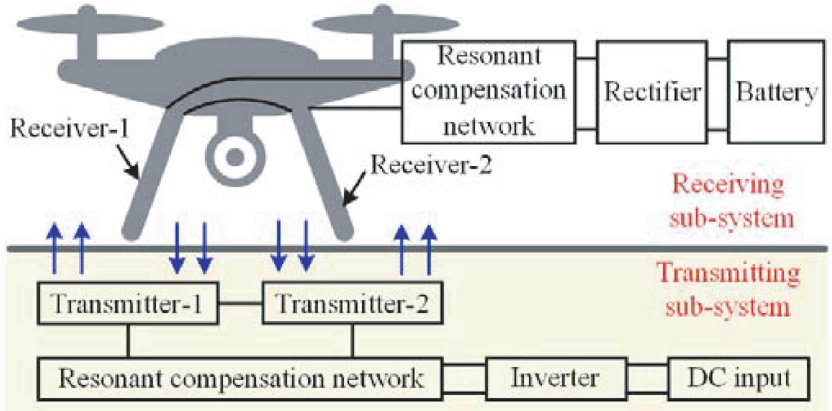

Figure 2. System circuit block diagram.

frequency excitation current is injected into the transmitters to generate alternating magnetic field above the landing platform. The receivers generate induced voltage under the action of the above magnetic field, which is delivered to the onboard battery for charging through compensation and rectifier.

2.2. Analysis of Coupling Principle

As shown in Fig. 3, each transmitter of the proposed magnetic coupler contains a bipolar coil with a back ferrite core. The two sub-windings in each bipolar transmitting coil are connected in reverse series to form a horizontal magnetic flux above the landing platform. As shown in Fig. 4, the horizontal magnetic flux can form an effective coupling with the receiver placed close to the vertical. In addition, the strong magnetic field area of the bipolar magnetic field is concentrated near the landing plane, which will not cause magnetic leakage interference to the UAV. The operation height of the main magnetic flux of the designed bipolar transmitter is 0.5 W. In order for the receiver to pick up the main magnetic flux to the maximum, the height H of the receiving coil needs to be greater than 0.5 W. Of course, the smaller the height of the receiving coil is, the lighter the weight is.

The receiving coil is made of hollow copper coated aluminum tubes as shown in Fig. 3. The aluminum tube can not only ensure the light weight of the landing gears, but also ensure high mechanical strength. In this way, there is no need to add additional coils to the UAV. Moreover, the aluminum

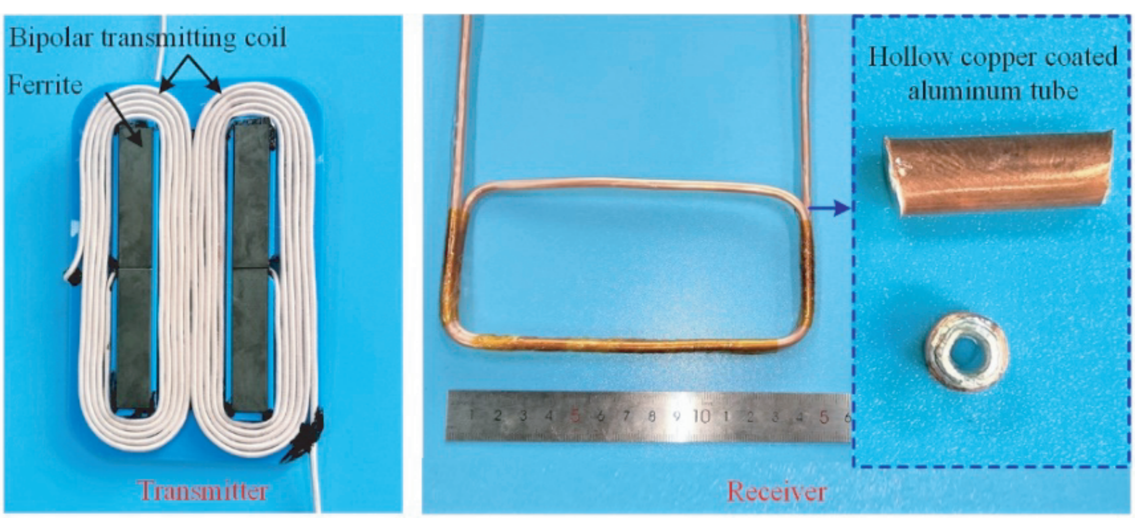

Figure 3. The transmitter and receiver of the proposed magnetic coupler.

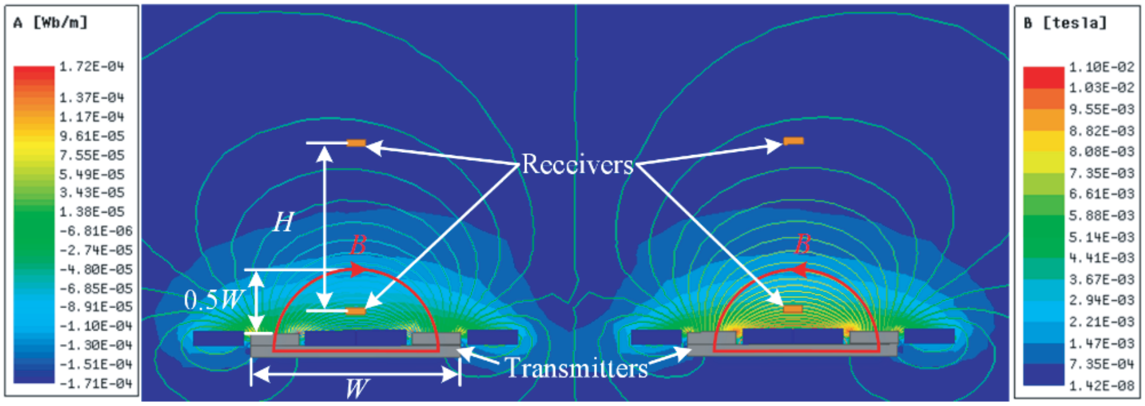

Figure 4. Magnetic field distribution.

landing gear is only 22 g. The key advantages of the proposed scheme are its low weight and low magnetic leakage interference.

The hollow copper-coated aluminum tube used by the receiver is shown in Fig. 5. The copper plating on the outside of the aluminum tube plays a main conductive role under the skin effect. The reason that copper plating is used instead of solid copper is the skin effect. This makes the most efficient use of the high conductivity copper, thereby reducing the alternating current (AC) resistance and reducing the weight of the receiver. The expression for the induced skin effect can be derived from Maxwell's equations, as shown in following equation

$$\begin{cases} H_x(y) = \dfrac{1}{2\pi R_1} e^{j\omega t - \sqrt{j\omega\sigma\mu - \omega^2\mu\varepsilon y}} \\ J_z(y) = \dfrac{\sqrt{\omega\mu\sigma} I}{2\pi(R_3 + h + w)} e^{j\omega t - \sqrt{2\omega\mu\sigma} y + \frac{\pi}{4}} \end{cases} \tag{1}$$

where y is the distance of electromagnetic field propagation from the surface of the tubular receiver to the interior, $H_x(0)$ the initial magnetic field strength on the surface of the tubular receiver, $J_z(y)$ the current density, σ the conductivity of the tubular receiver, ε the permittivity of the tubular receiver, I the induced current of the tubular receiver, h the thickness of copper layer, and w the thickness of aluminum layer.

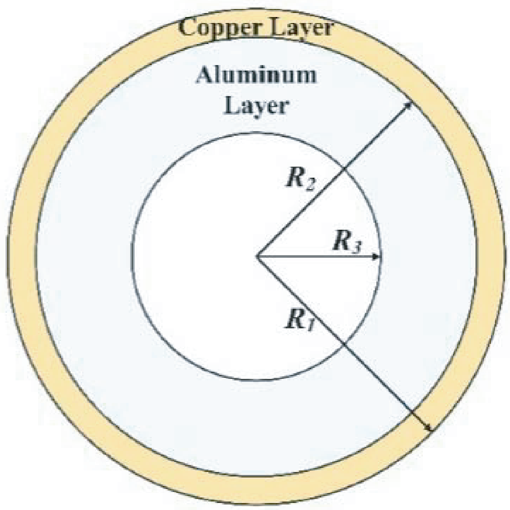

Figure 5. The hollow copper-coated aluminum tube structure.

The relationship between skin depth δ and alternating magnetic field frequency f is given by

$$\delta = \frac{1}{\sqrt{\pi f \mu \sigma}} \tag{2}$$

where μ is the magnetic permeability of the tubular receiver. For the receiver lightweight design, the hollow copper-coated aluminum tube should have limited wall thickness. From the above equation, it can be derived that the wall thickness of the tubular receiver should be designed to satisfy at least 4δ totally. 98.2% of the induced current will be transferred to the load side. The transfer current requirement and lightweight target are balanced well.

3. SYSTEM CIRCUIT DESIGN AND ANALYSIS

3.1. Circuit Topology

The developed UAV WPT system topology is shown in Fig. 6. The system is composed of voltage source full-bridge inverter, primary-side inductance-capacitance-inductance and secondary-side series compensation (LCC-S) compensation network, and full-bridge rectifier. U_{DC} is the input DC voltage, and L_T and L_R are the self-inductance of the transmitter and receiver, respectively. M is the mutual inductance. L_1 is the compensation inductance. C_1, C_2, and C_3 are compensation capacitors. R_L is the load resistance. U_o is the system output DC voltage.

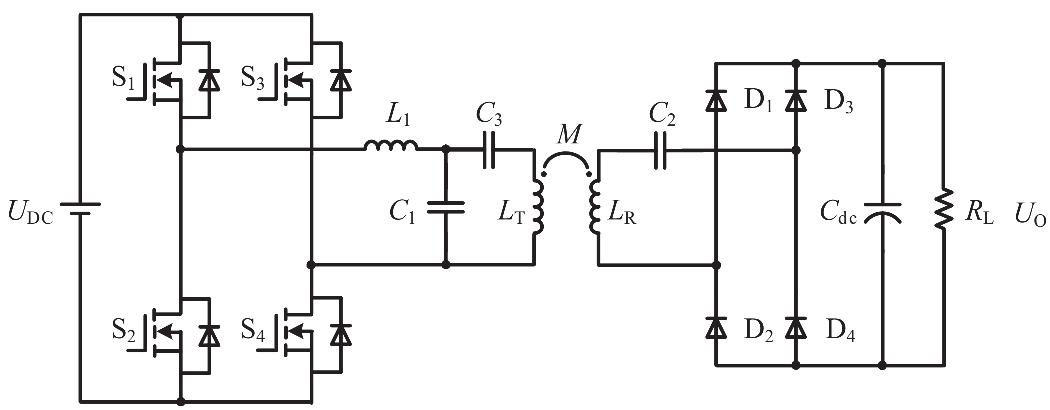

Figure 6. UAV WPT system circuit.

3.2. System Modeling and Analysis

There is a large air gap in the magnetic coupler, resulting in leakage inductance of both transmitter and receiver. In order to improve the transmission power and efficiency of the system, the compensation network parameter is designed by circuit resonant state, that is, the parameters of compensation elements should satisfy the following equation

$$\omega = \frac{1}{\sqrt{L_1 C_1}} = \frac{1}{\sqrt{\left(L_T - \frac{1}{\omega^2 C_3}\right) C_1}} = \frac{1}{\sqrt{L_R C_2}} \tag{3}$$

where ω is the system operating angular frequency.

The secondary resonant compensation network is a good band-pass filter. The fundamental harmonic of the output voltage of the inverter and the input voltage of the rectifier can be obtained by using the fundamental mode analysis method, which can be expressed as

$$\begin{cases} U_{\mathrm{IN}} = \dfrac{2\sqrt{2}}{\pi} U_{\mathrm{DC}} \\ U_{\mathrm{out}} = \dfrac{2\sqrt{2}}{\pi} U_O \end{cases} \tag{4}$$

According to Kirchhoff's Voltage Law (KVL), it can be obtained that the magnetizing current of the transmitter is

$$I_T = \frac{U_{\mathrm{IN}}}{j\omega L_1 + \frac{1}{j\omega C_1} // \left(j\omega L_T + \frac{1}{j\omega C_3} + Z_R\right)} \cdot \frac{\frac{1}{j\omega C_1}}{\frac{1}{j\omega C_1} + \left(j\omega L_T + \frac{1}{j\omega C_3} + Z_R\right)} \tag{5}$$

where Z_R is the reflection reactance, which is

$$Z_R = \frac{(\omega M)^2}{j\omega L_R + \frac{1}{\omega C_2} + R_{eq}} \tag{6}$$

where R_{eq} is the equivalent load resistance.

By substituting Equation (6) into Equation (5), the simplified magnetizing current model can be obtained as

$$I_T = \frac{2\sqrt{2}}{\pi} \frac{U_{\mathrm{DC}}}{\omega L_1} \tag{7}$$

Pickup voltage of receiver will be

$$U_R = \omega M I_T = \frac{2\sqrt{2}}{\pi} \frac{U_{\mathrm{DC}} M}{L_1} \tag{8}$$

Then, the system output voltage can be derived as

$$U_O = \frac{M}{L_1} U_{\mathrm{DC}} \tag{9}$$

4. EXPERIMENTAL VERIFICATION

4.1. Prototype Development

The developed UAV WPT prototype is depicted in Fig. 7, and the system parameters are listed in Table 1. Each transmitter winding consists of 5 turns of 0.1 mm × 400 litz wire. The receiver is made

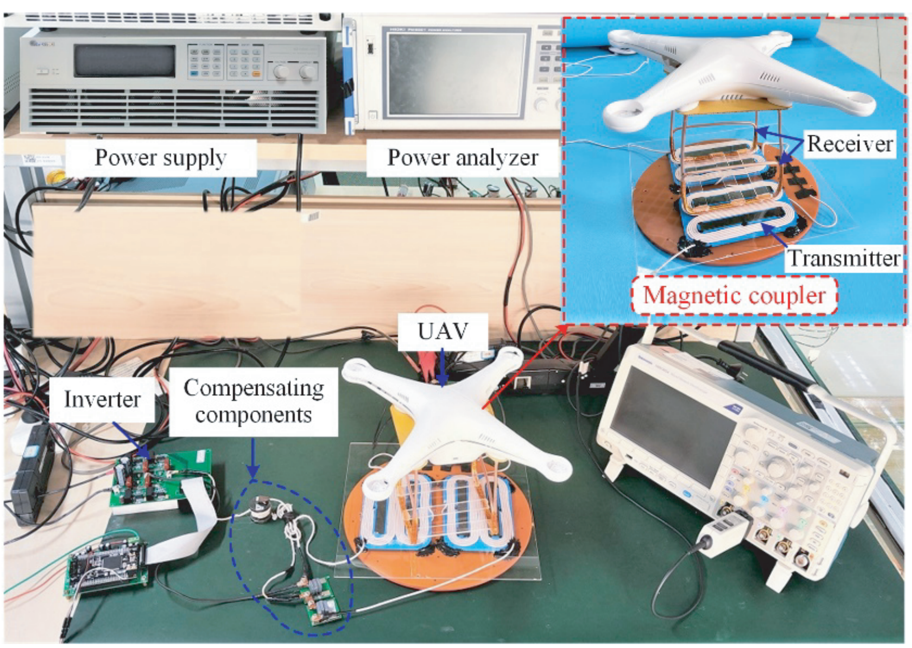

Figure 7. Experimental setup.

Table 1.

Parameters	Value	Parameters	Value
U_{DC}	150 V	L_1	10 µH
f	200 kHz	C_1	63 nF
L_T	30.6 µH	C_2	338 nF
L_R	1.87 µH	C_3	31 nF
M	2.41 µH	Weight of each receiver	22 g

of a hollow aluminum tube, having 1 mm thick walls and 0.2 mm copper plating. Each receiver has 1.75 turns.

4.2. Power Transmission Test

The power analyzer shown in Fig. 7 was used to obtain the input and output power of the UAV WPT system. The parameters are shown in Fig. 8. The output power of the system is 157 W, and the DC-DC efficiency is 80%.

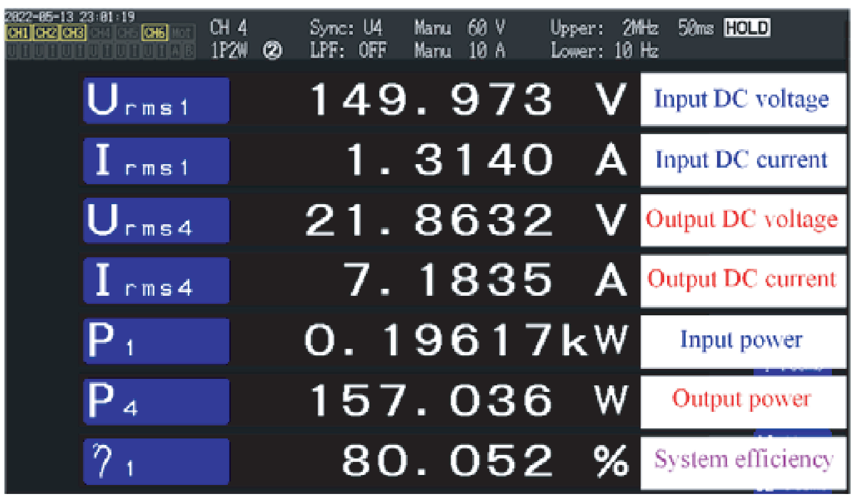

Figure 8. Power and efficiency test results.

Table 2. Performance comparison with previous works.

Reference	Frequency (kHz)	Efficiency (%)	Power (W)	Receiver weight (g)	Weight power density ratio (W/g)	Receiver material
[15]	300	30–90	70	78	0.897	Aluminum tube
[16]	250	77–80	32.48	94	0.345	Copper-coated aluminum tube
[17]	6780	70	100			Copper tube
This Work	200	80	157	$22 * 2$	3.568	Copper-coated aluminum tube

An overall comparison is made between the relevant performance parameters of this work and previous works in the references, and the parameters are shown in Table 2.

The comparison of the parameters in Table 2 shows that the coupling magnetic field distribution proposed in this paper has a high lightweight level with excellent weight power density ratio. This coupling structure is suitable for UAV wireless charging applications with conforming transmission power and efficiency.

5. CONCLUSION

In order to meet the future development needs of UAV's independent power supply, a novel UAV WPT system is proposed in this paper. Hollow copper-coated aluminum tubes are used to build the receivers, which also act as the landing gear of the UAV. Additional coils do not need to be attached to the UAV, thus reducing weight. The performance of the proposal is verified by a UAV WPT prototype. The system can deliver 157 W to the onboard load with a DC-DC efficiency of 80%. The weight power density ratio is 3.568 W/g. This coupling structure has high power density performance and achieves light weight.

REFERENCES

1. Sawadsitang, S., D. Niyato, P. Tan, et al., "Joint ground and aerial package delivery services: A stochastic optimization approach," *IEEE Transactions on Intelligent Transportation Systems*, Vol. 20, No. 6, 2241–2254, 2019.
2. He, T., Y. Zeng, and Z. Hu, "Research of multi-rotor UAVs detailed autonomous inspection technology of transmission lines based on route planning," *IEEE Access*, Vol. 7, No. 1, 114955–114965, 2019.
3. Kumar, N., D. Puthal, T. Theocharides, et al., "Unmanned aerial vehicles in consumer applications: New Applications in current and future smart environments," *IEEE Consumer Electronics Magazine*, Vol. 8, No. 3, 66–67, 2019.
4. Zhang, B., Q. Chen, G. Ke, et al., "Coil positioning based on DC pre-excitation and magnetic sensing for wireless electric vehicle charging," *IEEE Transactions on Industrial Electronics*, Vol. 68, No. 5, 3820–3830, 2021.
5. Khan, N., H. Matsumoto, and O. Trescases, "Wireless electric vehicle charger with electromagnetic coil-based position correction using impedance and resonant frequency detection," *IEEE Transactions on Power Electronics*, Vol. 35, No. 8, 7873–7883, 2020.
6. Cai, C., S. Wu, Z. Zhang, et al., "Development of a fit-to-surface and lightweight magnetic coupler for autonomous underwater vehicle wireless charging systems," *IEEE Transactions on Power Electronics*, Vol. 36, No. 9, 9927–9940, 2021.
7. Wu, S., C. Cai, W. Chai, et al., "Uniform power IPT system with quadruple-coil transmitter and crossed dipole receiver for autonomous underwater vehicles," *IEEE Transactions on Industry Applications*, Vol. 58, No. 1, 1289–1297, 2021.
8. Huang, S., T. Lee, W. Li, et al., "Modular on-road AGV wireless charging systems via interoperable power adjustment," *IEEE Transactions on Industrial Electronics*, Vol. 66, No. 8, 5918–5928, 2019.
9. Zhou, J., B. Zhang, W. Xiao, et al., "Nonlinear parity-time-symmetric model for constant efficiency wireless power transfer: Application to a drone-in-flight wireless charging platform," *IEEE Transactions on Industrial Electronics*, Vol. 66, No. 5, 4097–4107, 2019.
10. Arteaga, J. M., S. Aldhaher, G. Kkelis, et al., "Dynamic capabilities of multi-mhz inductive power transfer systems demonstrated with batteryless drones," *IEEE Transactions on Power Electronics*, Vol. 34, No. 6, 5093–5104, 2019.
11. Zhang, H., Y. Chen, C. H. Jo, et al., "DC-link and switched capacitor control for varying coupling conditions in inductive power transfer system for unmanned aerial vehicles," *IEEE Transactions on Power Electronics*, Vol. 36, No. 5, 5108–5120, 2021.

12. Song, K., P. Zhang, Z. Chen, et al., "A high-efficiency wireless power transfer system for unmanned aerial vehicle considering carbon fiber body," *2020 22nd European Conference on Power Electronics and Applications (EPE'20 ECCE Europe)*, 1–7, 2020.
13. Yang, C., Y. He, H. Qu, et al., "Analysis, design and implement of asymmetric coupled wireless power transfer systems for unmanned aerial vehicles," *AIP Advances*, Vol. 9, No. 2, 1–11, 2019.
14. Aldhaher, S. and P. D. Mitcheson, "500 W 13.56 MHz class EF push-pull inverter for advanced dynamic wireless power applications," *2019 IEEE PELS Workshop on Emerging Technologies: Wireless Power Transfer (WoW)*, 263–267, 2019.
15. Campi, T., S. Cruciani, F. Maradei, and M. Feliziani, "Innovative design of drone landing gear used as a receiving coil in wireless charging application," *Energies*, Vol. 12, 3483, 2019.
16. Cao, P., Y. Lu, C. Lu, et al., "A novel lightweight tubular receiver for drone wireless charging system," *Microwave Optical and Technology Letters*, 2022.
17. Lan, L., C. H. Kwan, J. M. Arteaga, D. C. Yates, and P. D. Mitcheson, "A 100 W 6.78 MHz inductive power transfer system for drones," *2020 14th European Conference on Antennas and Propagation (EuCAP)*, 1–4, 2020.
18. Campi, T., F. Dionisi, S. Cruciani, et al., "Magnetic field levels in drones equipped with Wireless Power Transfer technology," *Asia-pacific International Symposium on Electromagnetic Compatibility*, 544–547, 2016.
19. Park, B. P. J., Y. Shin, et al., "Wireless charging system using soft magnetic composite for unmanned aerial vehicle," *International Journal of Communications*, Vol. 2, No. 1, 59–62, 2017.
20. Song, C., H. Kim, Y. Kim, et al., "EMI reduction methods in wireless power transfer system for drone electrical charger using tightly coupled three-phase resonant magnetic field," *IEEE Transactions on Industrial Electronics*, Vol. 65, No. 9, 6839–6849, 2018.
21. Budhia, M., J. T. Boys, G. A. Covic, et al., "Development of a single-sided flux magnetic coupler for electric vehicle IPT charging systems," *IEEE Transactions on Industrial Electronics*, Vol. 60, No. 1, 318–328, 2013.
22. Cai, C., S. Wu, L. Jiang, et al., "A 500-W wireless charging system with lightweight pick-up for unmanned aerial vehicles," *IEEE Transactions on Power Electronics*, Vol. 35, No. 8, 7721–7724, 2020.
23. Wu, S., C. Cai, L. Jiang, et al., "Unmanned aerial vehicle wireless charging system with orthogonal magnetic structure and position correction aid device," *IEEE Transactions on Power Electronics*, Vol. 36, No. 7, 7564–7575, 2021.